

# Machine Learning Based Probe Skew Correction for High-frequency BH Loop Measurements

Yakun Wang, Song Liu, Jun Wang, *Member, IEEE*, Binyu Cui, *Student Member, IEEE*, and Jingrong Yang

**Abstract**—Experimental characterization of magnetic components has grown to be increasingly important to understand and model their behaviours in high-frequency PWM converters. The BH loop measurement is the only available approach to separate the core loss as an electrical method, which, however, is susceptible to the probe phase skew. As an alternative to the regular de-skew approaches based on hardware, this work proposes a novel machine-learning-based method to identify and correct the probe skew, which builds on the newly discovered correlation between the skew and the shape/trajectory of the measured BH loop. A special technique is proposed to artificially generate the skewed images from measured waveforms as augmented training sets. A machine learning pipeline is developed with the Convolutional Neural Network (CNN) to treat the problem as an image-based prediction task. The trained model has demonstrated a high accuracy in identifying the skew value from a BH loop unseen by the model, which enables the compensation of the skew to yield the corrected core loss value and BH loop.

**Keywords**—machine learning, BH loop measurement, power magnetics, instrumentation, probe skew

## I. INTRODUCTION

The characterization of core loss for high-frequency magnetic components (e.g. Fig. 1(a)) used in power conversion applications has been increasingly important to inform the design and virtual prototyping of power converters. The most common method for measuring high-frequency core loss is the two-winding BH loop measurement approach shown in Fig. 1(b), due to its capability of separating the core loss (i.e. excluding the copper loss) and suitability for rapid testing under high-frequency excitations without the need for reaching a thermal equilibrium, compared to the calorimetric approaches.

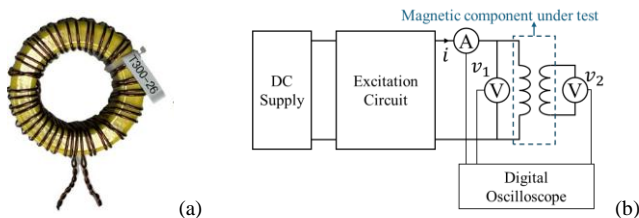


Fig. 1. (a) magnetic component for high-frequency power electronics applications (b) Two-winding BH loop measurement

However, the most challenging aspect of the two-winding method is the phase discrepancy error caused by the different propagation delays between the voltage and current probes, known as the skew - the probe skew can lead to a distorted BH loop resulting in up to  $\pm 200\%$  of error in the measured core loss [1]. Conventionally, probe skew can only be calibrated through deskew tools, such as Keysight U1880A or Lecroy DCS025, which are designed to show a pair of voltage and current waveforms that are in phase to the probes. However, these tools cannot eliminate the skew due to physical imperfections on the hardware such as the inevitable parasitics in the circuits. Incorrectly measured magnetic core loss will misinform the

design process of power electronic systems, which can lead to wrongly sized cooling components and potential failure of the converter systems in safety-critical applications, e.g. electric passenger cars.

Alternatively, methods have been proposed to alter the measurement and excitation circuits to minimize the impact of the probe skew. In [2], [3], the concept of reactive voltage cancellation is proposed to avoid capturing a pair of voltage and current waveforms that are almost in a  $90^\circ$  phase difference by placing reference components into the testing circuit. This concept's limitation is the requirement of the reference components which need to be precise matches to the device under test. [4] proposes to place a small capacitor in the testing circuit to induce a 'notch' in the measured voltage waveform which contains the information of probe skew to enable the correction. However, this approach is still challenging to practically implement as it requires a dedicated design of testing circuits with a swappable capacitor which is invasive for the main power circuit.

This article proposes a novel and timely solution to solve the probe skew problem in the two-winding BH loop measurement through a machine learning and data-driven approach, which does not require a local piece of hardware, i.e. a de-skew tool. The key concept is to establish a model that learns the mapping between the shape irregularity of the measured BH loop and the degree of skew, which is realized by a convolutional neural network (CNN) through a supervised learning process. For the first time, the correlation between the probe skew and the shape irregularity is revealed and evaluated in this work.

A training pipeline is developed and applied to the open-source MagNet dataset (<https://github.com/minjiechen/magnetchallenge>), which is a rich database of experimentally measured waveforms, along with a data augmentation technique to embed artificial skew values to create the training data. Fundamentally, the proposed machine learning approach treats the skew correction problem as an image recognition task. It does not suffer from the imperfection of a local de-skew tool, assuming the original training data is skew-free. The effectiveness of the proposed approach is validated on a testing set randomly selected from the dataset.

## II. PROBE SKEW IN BH LOOP MEASUREMENT

### A. Impact of probe skew on core loss measurement

To obtain the core loss, the two-winding method shown in Fig. 1 includes two steps: (1) measuring out the voltage  $v_2$  and current  $i$  waveforms and (2) converting the time-series of the electrical waveforms into flux density  $B$  and field strength  $H$ , then, forming a BH loop where the area is the core loss.

$$B(t) = \frac{1}{N_2 A_e} \int_0^t v_2(t) dt \quad (B(0) = 0) \quad (1)$$

$$H(t) = N_1 \cdot i(t) / l_e \quad (2)$$

Where  $N_1$  is the number of turns of the main winding of the inductor;  $N_2$  is the number of turns of the flux-sensing winding;  $A_e$  is the effective cross-section area of the core;  $l_e$  is the effective magnetic path length of the core. In this process, the physical probe skew can be mimicked by shifting the measured waveforms horizontally along the time axis. In this work, the  $H(t)$  waveform is the signal to be shifted to mimic the phase skew since it is directly proportional to the current waveform (2). This approach also echoes the fact that the voltage probe is typically the reference point in a probe calibration process. This technique enables the generation of data points with an artificial skew time.

The impact of the probe skew on measured core loss is shown in Fig. 2, treating the original data as the ground truth. It can be seen that the core loss deviation under one operating condition is in a linear relationship against the skew time in nanoseconds, which aligns with the findings reported in [1]. In practice, the delay of the current probe can range from a few to hundreds of nanoseconds. This linear relationship enables the correction of core loss once the skew time is known.

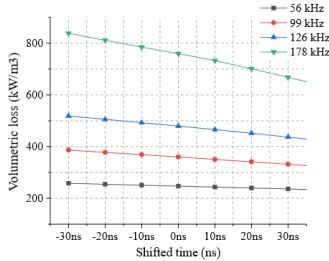


Fig. 2. 3C90 core loss ( $\Delta B = 176$  mT) with imposed skew time

### B. Shape irregularity in BH loops due to probe skew.

To correct the probe skew, the conventional approach is to supply a voltage (typically with sharp rising/falling edges) on a non-inductive resistor to generate a pair of voltage/current waves that are physically in phase so that the skew caused by the probe can be identified on an oscilloscope, which is the principle of the de-skew tools. As a fundamentally different approach, this work proposes to (1) convert the voltage/current waveform measured from a magnetic component into the BH domain (2) identify the shape irregularity in the BH loops as a feature that links to the probe skew. Fig. 3 shows a BH loop measured experimentally through a Triple Pulse Test (TPT) procedure [5] on a ferrite core T184-26. Fig. 3(a) is the BH trajectory treated as the ground truth with the probes calibrated through a de-skew tool U1880A. Fig. 3(b) shows the BH loop once an artificial skew of 1.25 milliseconds is applied by shifting the data points of the current  $I$  (equivalently the  $H$ ) on the time axis. The distortion of the shape is visually noticeable in this case, and as a result, the core loss obtained from this loop sees a +123% difference compared to the original BH loop. This example demonstrates the dependency between the skew and the BH loop shape irregularity, which enables a pattern recognition technique based on machine learning to be developed for this problem.

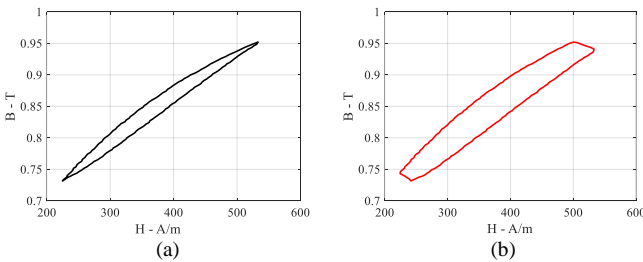


Fig. 3. Illustration of the shape irregularity associated with the probe skew (a) original BH loop (b) distorted BH loop with a skew of 1.25 ms

To further show the effect of skew, Fig. 4 illustrates a set of BH loops with both positive (delaying the current) and negative (delaying the voltage) artificial skews. As can be observed, with a negative skew, the BH loop area shrinks, and the trajectory shows incorrect crossovers. With a positive skew, which is the more common case where the current probe suffers more delays, the BH loop area expands, and the trajectory shows a ‘flat top’. These observations correspond to the trend in loss value shown in Fig. 2 in both directions.

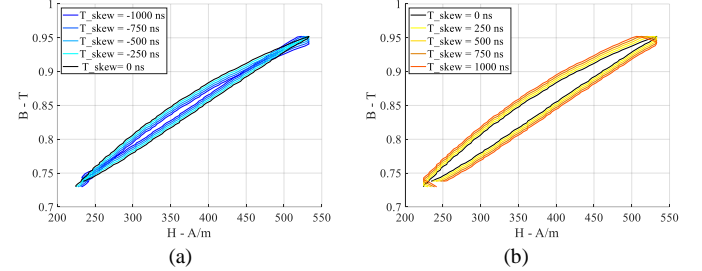


Fig. 4. Trend of BH loop shape distortion associated with various skew values (a) a negative skew (current leading) (b) a positive skew (current lagging). The colour gradient shows the trend of distortion.

## III. MACHINE LEARNING-BASED CORRECTION APPROACH

### A. Overall pipeline

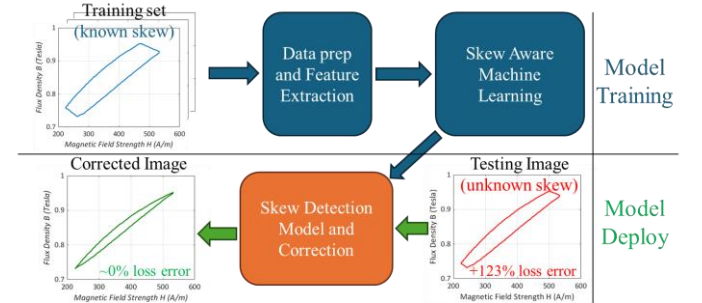


Fig. 5. Illustration of the proposed ML approach for skew detection

In recent years, CNN [6] [7] as a computer vision neural network architecture has been widely used in various sectors due to its capability to explore patterns in image data. For example, CNNs have been applied in healthcare applications for disease diagnosis [8], autonomous driving for object recognition [9], security for facial recognition [10], and agriculture for monitoring crop health and detecting plant diseases [11]. Inspired by the superb image recognition capability of CNNs, we propose a hyperparameter-free CNN approach for detecting the skew from high-frequency BH loop measurements. The high-level workflow of this approach is illustrated in Fig. 5. In the training stage, the training set is constructed using BH loops with known skew values. A supervised training process is then applied to fit a CNN-based skew detection model. As the outcome, the trained model can then be used to predict/detect the unknown skew (in degrees) associated with an unseen testing BH loop image. Using the detected skew value, the input BH loop and its associated core loss are then corrected/recalibrated to produce the un-skewed final output. In this work, the open-sourced MagNet database is used to construct training and testing sets [12].

### B. Data preprocessing

The MagNet dataset contains the raw time-series data of  $B$  and  $H$  from different materials. They are structured as

$$\begin{cases} B = [B_{t_1} \dots B_{t_N}] \\ H = [H_{t_1} \dots H_{t_N}] \end{cases} \quad (3)$$

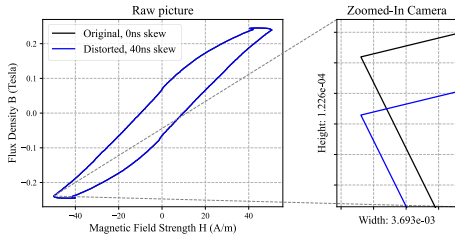


Fig. 6. Comparison of the shape irregularity with the original BH loop (black) and distorted BH loop with a skew of 40 ns (blue) from 3C90

By sequentially connecting the B-H coordinates ( $H_{t_n}, B_{t_n}$ ) according to their index  $t_n$ , we can transform the raw time-series data into a “loop-shaped curve”. These curves are referred to as the BH loops. This work uses the BH loops as the inputs for a machine-learning model to predict the skew. The data from the MagNet database are extracted and preprocessed as:

1. Preparing the dataset: targeting representative power electronics applications, the dataset used in this work is extracted from the MagNet database by applying the following filters without any bias (1) triangular flux waveform (2) temperature at 25 °C (3) DC bias at 1A/m.

2. Waveform interpolation: The original dataset consists of  $B$  and  $H$  as time series. Each time series is stored as a 1024-dimensional vector. While the raw data has only 1024 points per cycle, linear interpolation is performed to expand the data points by 1000 times more to achieve a higher resolution. This operation effectively achieves a resolution of  $3.5 \times 10^{-4}$  degrees.

3. Data augmentation: To create the training set with artificial skew values, each BH loop is augmented by an artificially imposed skew, which is realized by shifting the indexes of the  $H$  sequence. For example, if the original time indexes are  $[t_1, t_2, t_3, \dots]$ , the shifted indexes are  $[t_1 + \delta, t_2 + \delta, t_3 + \delta, \dots]$  and  $\delta$  is the artificial skew index. If the range of  $\delta$  is set as  $[-20, +20]$ , one BH loop from the database can be expanded to a set of 41 BH loops each with a known skew value, including the original loop which has a skew of zero degrees.

4. Zooming-in: It is observed that a small skew (e.g. by 0.01 degrees) will lead to a distortion that is almost visually unidentifiable (see Fig. 6), implying that it may be difficult for CNNs to capture the visual differences in the image. To address this, an additional zoom-in camera is set at the bottom left of a BH loop, centered at the coordinate with the minimum value of  $H$ . This zoomed-in image typically includes patterns which are more recognizable and captures fine details caused by a small skew better. The zoomed image is placed next to the original BH loop as a part of the input image (see Fig. 7(b)).

5. Extra Scale Information: The size of the BH loop varies considerably under different operating conditions (see Fig. 7. (a)), thus, an automatic scaling and centering function is applied to each BH loop to obtain a reasonably sized training image. To factor in this automated scaling, the minimum and maximum

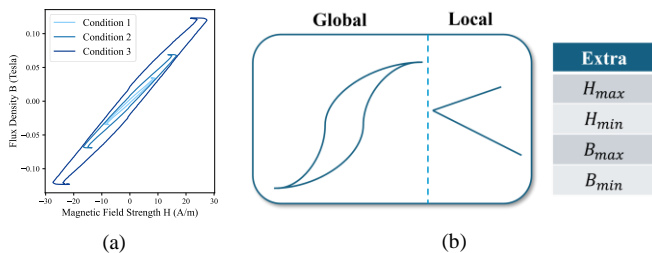


Fig. 7. Illustration of (a) different sizes of BH loops and (b) the input data to the neural network: the original BH loop, the zoomed-in view and four scalars

values of  $B$  and  $H$  are also included as a part of the input, to indicate the actual scale of the original image ensuring that this information is not lost during the training process.

### C. The architecture of CNN

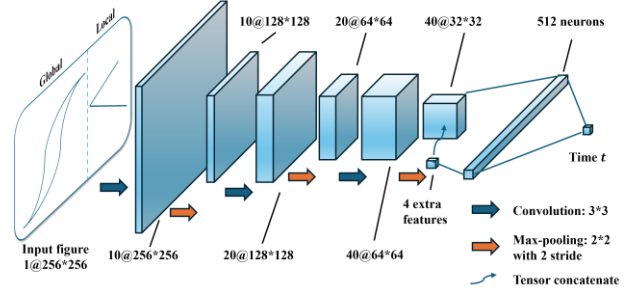


Fig. 8. Illustration of the CNN architecture

Fig. 8 summarizes the architecture of the proposed CNN model. The input picture is resized to 256×256 pixels (including both the original image and the zoomed-in view) to improve the computational efficiency. There are 8 layers in the CNN in total. Particularly, it comprises three convolutional layers, each followed by a max pooling layer. The first convolutional layer employs 10 filters with a kernel size of 3×3, stride of 1, and padding of 1. The second and third convolutional layers use 20 and 40 filters, respectively, maintaining the same kernel size and stride parameters. Following the last pooling layer, the output is flattened and then concatenated with a tensor storing four additional scale information (see Fig. 7.(b)). This combined feature vector is processed by two fully connected layers dedicated to the regression task. The first fully connected layer maps the input data to 512 hidden units, followed by a leaky ReLU activation function with a 0.01 negative slope. The second fully connected linear layer directly produces a single scalar output representing the predicted skew time.

### D. Training and testing

By applying the filters stated, two sub-datasets are extracted from the MagNet database, which are described below. Two CNN models are trained for the 3C90 and N87 materials, which are the two most common and representative soft magnetic materials, to evaluate the validity and the general applicability of the proposed approach.

Table I Datasets used for training and testing.

	$\Delta B$ (pk-pk, T)	Frequency (Hz)	Operating Points
3C90	[0.0215, 0.5524]	[56330, 446430]	1197
N87	[0.0213, 0.5498]	[49970, 446430]	1879

Following the data augmentation process, the total number of images is expanded to  $1197 \times 41 = 49077$  for the 3C90 set and 77039 for the N87 set. The training and the testing operation points are randomly selected. The loss function is defined by

$$L(\theta) = \frac{1}{N} \sum_{i=1}^N |t_i - t'_i(\theta)|^2 \quad (4)$$

where  $N$  is the training sample size,  $t_i$  is the target skew, artificially imposed during the data preprocessing and  $t'_i(\theta)$  is the model prediction. The CNN is trained using ADAM optimizer by minimizing the loss  $L(\theta)$  through backpropagation techniques with a learning rate set to  $2.5 \times 10^{-3}$ . Training of the CNN was performed in 50 epochs. For the 3C90 set, a batch size of 500 is used, with a training-to-testing ratio of 1000:197. For



the N87 set, a batch size of 400 is used, with a training-to-testing ratio of 1600:279.

#### IV. EVALUATION AND VALIDATION

To quantitatively assess the performance of the proposed model, the relative error against the testing set for the two core materials 3C90 and N87 is shown below, containing  $197 \times 41 = 8077$  and 11439 testing data points, respectively.

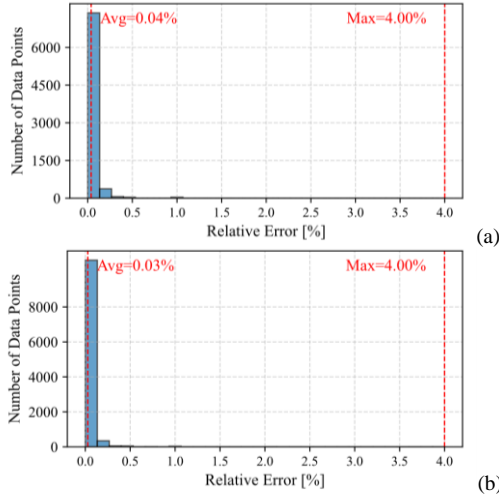


Fig. 9. Relative error distributions of identified skew (a) 3C90 (b) N87

Fig. 9 shows that the proposed method achieves remarkably low relative errors, i.e. 0.04% and 0.03%, respectively. The maximum relative error is at 4.00% for both datasets, implying the validity and the consistent performance of the CNN model across different materials and the generality of the proposed approach. The validation on the MagNet database demonstrates that the proposed model can successfully capture the feature of the time skew from BH loops at a resolution of  $3.5 \times 10^{-4}$  degrees (i.e.  $\sim 0.02$  nanoseconds for the case with  $\sim 50$  kHz).

Fig. 10 provides a comprehensive evaluation of the relative error distributions of core loss before and after the skew correction, further demonstrating the validity of the proposed approach in the engineering context. The relative errors of the uncalibrated core loss points, indicated by red markers, show significant deviations across 5 frequencies arising from the imposed skew. After calibration, the relative errors of the new core loss, represented by blue markers, are significantly lower, with nearly all deviations shrinking to zero. Furthermore, Fig. 10(a) illustrates that the proposed CNN model effectively reduces the relative deviations for 3C90 across various frequency levels, verifying its robustness. Similarly, Fig. 9(b) confirms that the method is transferable to N87, achieving near-zero calibrated deviations across a diversified range of operation points. These results demonstrate the general applicability and accuracy of the proposed CNN-based correction method in de-skewing the high-frequency BH loop measurements across different materials and operating points.

#### V. CONCLUSION

This work proposes a novel method to identify and compensate the probe skew in a measured BH loop to correct the core loss data for tested magnetics exposed in PWM waveforms. For the first time, the correlation between the probe skew and the shape irregularity is revealed and evaluated. A vision-based shape-aware calibration algorithm is then developed to capture the complex patterns embedded in the shape irregularity of BH loops. It is able to accurately identify prob skews in nanoseconds using these complex correlation. The

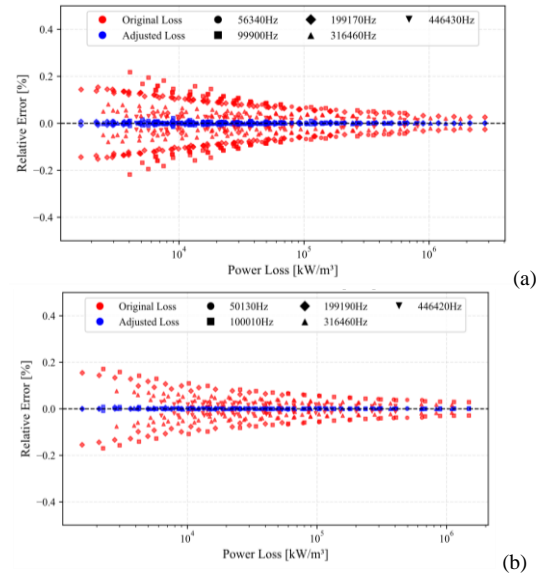


Fig. 10. Relative deviation of core loss (a) 3C90 (b) N87

algorithm is trained on the open-source MagNet database, which is an experimentally measured dataset. The proposed ML-based method is evaluated against testing sets on two common core materials 3C90 and N87. The evaluations have demonstrated that the proposed approach is effective, accurate, and generalizable. This approach can serve as a software alternative to the hardware-based de-skew tools for high-precision BH loop measurements.

#### REFERENCES

- [1] N. Rasekh, J. Wang, and X. Yuan, "A new method for offline compensation of phase discrepancy in measuring the core loss with rectangular voltage," *IEEE Open J. Ind. Electron. Soc.*, vol. 2, no. April, pp. 302–314, Apr. 2021.
- [2] M. Mu, Q. Li, D. J. Gilham, F. C. Lee, and K. D. T. T. Ngo, "New core loss measurement method for high-frequency magnetic materials," *IEEE Trans. Power Electron.*, vol. 29, no. 8, pp. 4374–4381, 2014.
- [3] D. Hou, M. Mu, F. C. Lee, and Q. Li, "New high-frequency core loss measurement method with partial cancellation concept," *IEEE Trans. Power Electron.*, vol. 32, no. 4, pp. 2987–2994, 2017.
- [4] L. Yi, M. McTigue, D. Gines, B. Doerr, and J. Moon, "Minimally Invasive Direct In-Situ Magnetic Loss Measurement in Power Electronic Circuits," *IEEE Trans. Power Electron.*, vol. 38, no. 11, pp. 14334–14344, Nov. 2023.
- [5] J. Wang, X. Yuan, and N. Rasekh, "Triple Pulse Test (TPT) for characterizing power loss in magnetic components in analogous to Double Pulse Test (DPT) for power electronics devices," in *IEEE Proc. Annual Conference of the IEEE Industrial Electronics Society (IECON)*, 2020.
- [6] Y. LeCun, K. Kavukcuoglu, and C. Farabet, "Convolutional networks and applications in vision," in *Proceedings of 2010 IEEE International Symposium on Circuits and Systems*, May 2010, pp. 253–256.
- [7] Y. Lecun, L. Bottou, Y. Bengio, and P. Haffner, "Gradient-based learning applied to document recognition," *Proc. IEEE*, vol. 86, no. 11, pp. 2278–2324, Nov. 1998.
- [8] G. Litjens *et al.*, "A survey on deep learning in medical image analysis," *Med. Image Anal.*, vol. 42, pp. 60–88, Dec. 2017.
- [9] C. Chen, A. Seff, A. Kornhauser, and J. Xiao, "DeepDriving: Learning Affordance for Direct Perception in Autonomous Driving," presented at the Proceedings of the IEEE International Conference on Computer Vision, 2015, pp. 2722–2730.
- [10] Y. Taigman, M. Yang, M. Ranzato, and L. Wolf, "DeepFace: Closing the Gap to Human-Level Performance in Face Verification," presented at the Proceedings of the IEEE Conference on Computer Vision and Pattern Recognition, 2014, pp. 1701–1708.
- [11] A. Kamilaris and F. X. Prenafeta-Boldú, "Deep learning in agriculture: A survey," *Comput. Electron. Agric.*, vol. 147, pp. 70–90, Apr. 2018.
- [12] H. Li *et al.*, "How MagNet: Machine Learning Framework for Modeling Power Magnetic Material Characteristics," *IEEE Trans. Power Electron.*, vol. 38, no. 12, pp. 15829–15853, Dec. 2023.